Computer Simulations of Composite Maps for Detection of Atrial Fibrillation Mechanisms

Ozan Özgül[1], Victor G. Marques [1], Ben Hermans[1], Arne van Hunnik[1], Sander Verheule[1], Ulrich Schotten[1], Ali Gharaviri[2], Simone Pezzuto[3], Angelo Auricchio[3], Pietro Bonizzi[4], Stef Zeemering[1]

[1] Department of Physiology, Maastricht University, The Netherlands
[2] Centre for Cardiovascular Science, University of Edinburgh, Edinburgh, United Kingdom
[3] Center for Computational Medicine in Cardiology, Euler Institute, Università della Svizzera Italiana, Lugano, Switzerland
[4] Department of Advanced Computing Sciences, Maastricht University, The Netherlands

Abstract

Localized AF drivers with repetitive activity are candidate ablation targets for patients with persistent atrial fibrillation (AF). High-density mapping electrodes cover only a fraction of the atria but combining sequential recordings could provide a more comprehensive picture of common repetitive atrial conduction characteristics and enable AF driver localization. We developed a novel algorithm to merge overlapping local activation maps into larger composite maps by linking repetitive patterns detected in neighboring locations with similar conduction directions and cycle lengths. Regions exhibiting high curl, divergence and heterogeneity in composite maps were marked as candidate reentry locations and were compared to those estimated through phase singularities and cycle length coverage maps from the individual recordings. The proposed algorithm led to better estimates of the underlying source density (sensitivity: 0.88/0.87/0.79, specificity: 0.85/0.85/0.68 for stable reentry, meandering reentry, and collision, respectively), compared to the maps from individual recordings (sensitivities 0.85/0.70/0.65 and 0.84/0.86/0.51, specificities 0.86/0.70/0.64 and 0.85/0.87/0.50 for phase singularity and CL coverage, respectively).

1. Introduction

Many localized mechanisms have been described as possible perpetuators of AF episodes; such as, functional reentries (rotors), transmural breakthroughs or focal activity [1]. Regardless of the underlying mechanism, AF drivers are expected to entrain their vicinities and exhibit repetitive propagation that is observed through intracardiac recordings [2]. This repetitive activity, however, cannot be visualized over the entire atrium due to the limited coverage of high-density catheters [3]. To address this problem, we developed a tool to link sequential repetitive atrial activation patterns (RAAPs) into larger maps- composite maps- that reflect the underlying conduction with high spatial resolution as well as a high coverage. This work aims to quantify in-silico local reentry detection performance of composite maps in comparison with individual analysis of sequential maps.

2. Methods

2.1. Dataset

AF was simulated in a highly detailed three-dimensional model of the human atria, including atrial wall thickness, intra and inter-atrial structures and realistic electrophysiology corresponding to AF patients [4]. Three AF driver scenarios were simulated: a stable reentry, a meandering reentry, and two colliding reentries. Unipolar electrograms were sequentially recorded from 30 overlapping locations on the left posterior wall (4x4 grid, 3mm spacing, 230 to 800 ms). Phase singularities obtained from the transmembrane potentials were used to track the position of reentry cores over time.

2.2. Detection of Repetitive Atrial Activation Patterns During AF

RAAP detection methodology is described in [2]. Briefly, local activation times were annotated using a probabilistic template matching approach and transformed into activation phase signals by activation phase interpolation. Each time-point was represented by the activation phase snapshot of all electrodes at that time instant. Time intervals in which similar sequences of phase snapshots appeared for more than two consecutive cycles were marked

as RAAP intervals. RAAPs were represented by the preferred conduction direction vectors of their electrodes which were calculated by averaging conduction velocity vectors during the time course of the analyzed RAAP. Electrodes that not dot show high directional preferentiality (i.e. a circular variance less than 0.5) were excluded from the analysis.

2.3. Repetitive Pattern Linking and Source Detection Algorithms

Repetitive patterns detected on different regions, e.g. $RAAP_1$ and $RAAP_2$, were stitched together using a set of rules (Fig. 1, left):
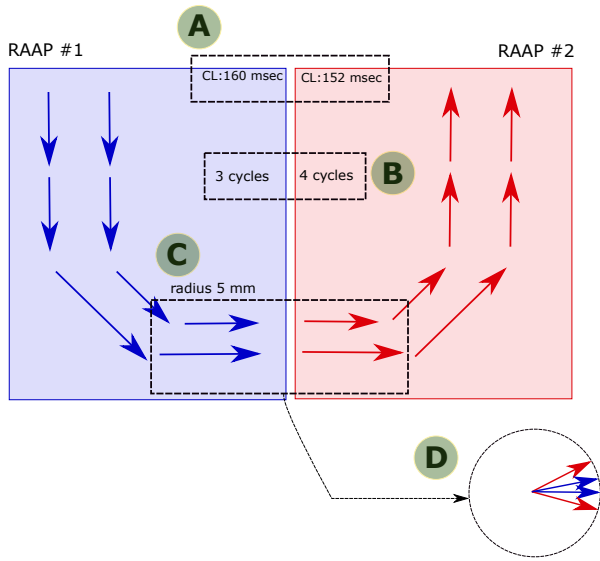

Figure 1. RAAP linking approach

A) **AF Cycle Length (AFCL) Coherence**: AFCLs associated with $RAAP_1$ and $RAAP_2$ should be at most 10% apart. This is based on the assumption that the AFCLs should not change significantly among neighbouring sites.
B) **Number of Cycles**: $RAAP_1$ and $RAAP_2$ should both be present at least for three consecutive cycles which ensures that the patterns are sufficiently repetitive and provides algorithmic efficiency by omitting shorter, transitory patterns.
C) **Distance**: Recording locations of $RAAP_1$ and $RAAP_2$ should be sufficiently close- there should be at least one electrode from each recording site which is within 0.5mm radius of each other.
D) **Preferential Directions**: Preferential conduction direction vectors associated with electrodes that are sufficiently close (see C) point similar directions-cosine of angles between vectors should be larger than 0.5.

We evaluated each identified RAAP pair according to these rules and consequently, a network of linked RAAPs was obtained. We represented this network as an undirected graph and extracted the largest connected component as the composite map associated with the data set.

Generated composite maps exhibited preferential conduction directions for an extended region of atria and could be processed to localize AF driver activities - e.g. local reentries. To that end, we utilized three vector field operators (Fig. 2): (i) Divergence: the volume density of the outward flux of a vector field around a given point. (ii) curl: the circulation density at each point of the vector field, (iii) Heterogeneity: norm of the average of all vectors within a radius R, reflecting how heterogeneous the vector directions are. We defined a metric, composite map source score (CMSS) based on these three operators:

$$CMSS(x,y,z) = max(C_{xyz}, D_{xyz}) \cdot H_{xyz} \quad (1)$$

with C_{xyz}, D_{xyz} and H_{xyz} being curl, divergence and heterogeneity values at the atrial surface position (x,y,z). Choosing the maximum of the curl and divergence provides capturing reentries with different propagation characteristics while multiplication with the heterogeneity had a smoothing effect.
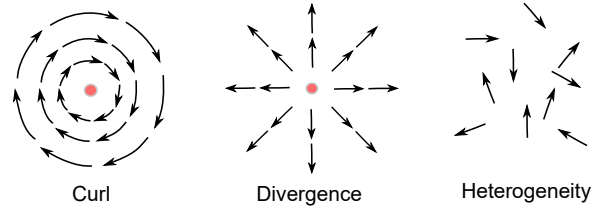

Figure 2. Curl, divergence and heterogeneity operators for vector field analysis.

Source distribution maps obtained with the CMSS method and two other sequential reentry detection methods were compared as follows: Maps were binarized with a threshold and sensitivity/specificity scores were calculated and contrasted. Threshold values were individually set for each technique such that the combination of the resulting sensitivity and specificity scores (F-scores) were maximized.

We have also quantified the dependency of the composite mapping algorithm to the mapping density- coverage of the atria. For this, random subsets of the recordings, varying from 0 to 50% of the measured locations, were eliminated from the analysis. This was repeated 100 times, and sensitivity and specificity values were calculated for each epoch to explore changes in reentry detection performance.
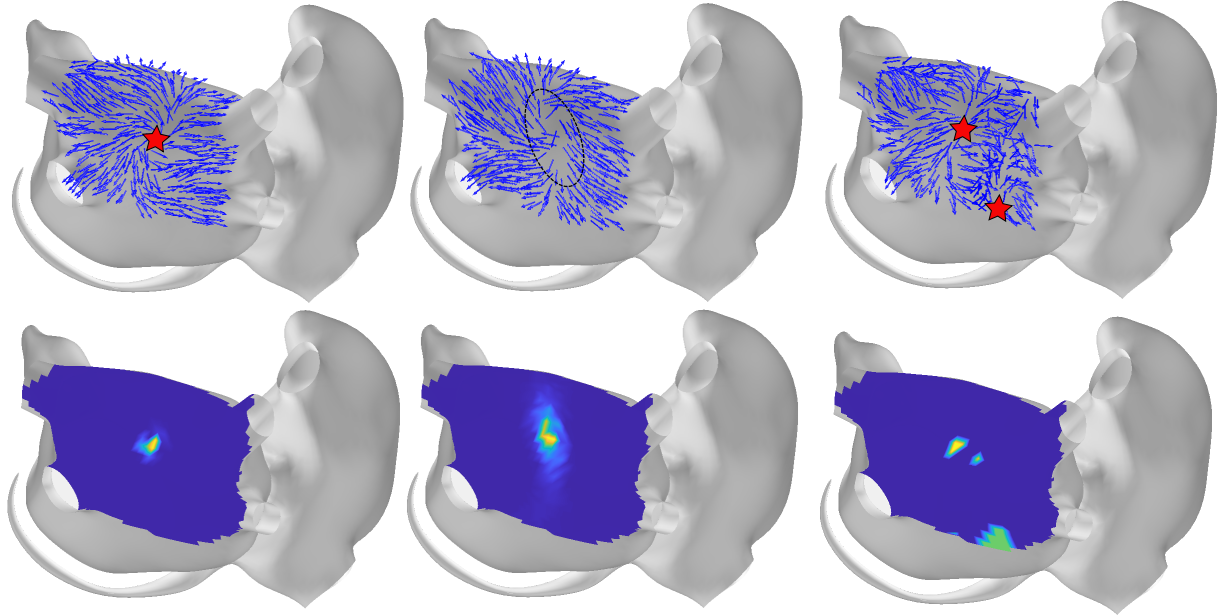
Figure 3. Examples of generated composite maps (top) and CMSS maps (bottom) for (left) stable reentry, (middle) meandering reentry, (right) two colliding reentries. Stars mark reentry cores.

3. Results

Composite maps and CMSS maps for three different types of local reentries were generated: stable, meandering and colliding (see Fig. 3). For the stable local reentry (Fig. 3, left), generated composite map exhibited a rotating pattern around a single point which was in agreement with center of the simulated stable reentry. In this case, CMSS map showed a sharp peak on that point. In the meandering reentry case (Fig. 3, middle), associated composite map had a lower arrow density around the center, and the CMSS map marked a broader area spanning the trajectory of the meandering reentry. In more complex case of a wave collision (Fig. 3,right), resulting composite maps captured the source activity with parts of the wave collision artifacts. Table 1 depicts the sensitivity and specificity values for each technique. In each scenario, CMSS achieved better sensitivity. This was more pronounced in the collision case where phase singularity performed poorly while cycle length coverage did hardly better than the random guess. The dependency of the composite mapping algorithm to the mapping density was summarized in Fig. 4. Both sensitivity and specificity values dropped approximately 20% when half of the sequential recordings were randomly removed.

4. Discussion

Generated composite maps reflected wave propagation of the underlying pattern in each simulated case. Detection
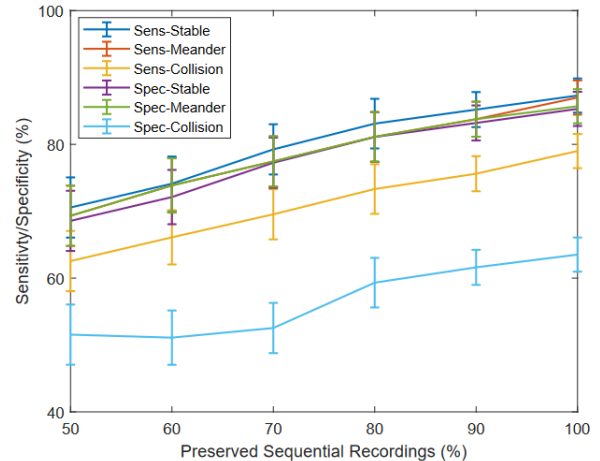

Figure 4. Sensitivity/specificity scores upon changing mapped density values.

of reentries in these maps outperformed widely used sequential reentry detection techniques, indicating possible benefits of high-coverage composite mapping of sources for ablation target detection.

While RAAPs were stable and long-termed in our simulations, clinical recordings may present more chaotic activation patterns and lower number of short-lived RAAPs which might complicate both RAAP detection and linking stages. Nevertheless, there is increased evidence of the

Table 1. Sensitivity/specificity values of different methods.

Pattern Type	CMSS	Phase Singularity	Cycle Length Coverage
Single Reentry	0.88/0.85	0.85/0.86	0.84/0.85
Meandering Reentry	0.87/0.85	0.70/0.70	0.86/0.87
Collision	0.79/0.68	0.65/0.64	0.51/0.50

presence of stable RAAPs during human AF [5][6], which could be visualized and analyzed with a similar approach as proposed here. Future studies should include clinical recordings to evaluate the applicability of the technique for guiding ablation.

A limitation of the composite mapping is increased mapping time due to the dense mapping required for a detailed map. Our results indicated that the sensitivity and specificity of the algorithm could withstand randomly-introduced decreased mapping density. Although this was a positive evidence for the applicability of composite mapping in clinical environment, electrophysiologists do not randomly select mapping locations and focus on particular anatomical sites instead. Therefore, our way to quantifying reduced mapping density might be an oversimplification and should be extended.

Proposed CMSS metric exploited vector fields of the generated composite maps and achieved very high sensitivity and specificity scores for the stable and meandering reentries, but under-performed in wave collision case. In collision scenario, the drop in specificity was due to the false positive detections in the vicinity of the collision zones where both electrogram morphologies and the preferential conduction vectors presented high complexity. On the other hand, lower sensitivity was introduced by the challenges in capturing the second reentry in the vicinity of right inferior pulmonary vein which was only partially mapped. The meandering reentry case highlighted the advantages of using composite maps: even though the rotor tip of the meandering region showed low repetitive activity, a composite map could still capture the overall pattern by linking the peripheral wave directions. On the other hand, competing techniques were affected more severely by propagation pattern characteristics: Meandering of a reentry obstructed emergence of phase singularities. Similarly, cycle length coverage metric prioritized collision zones which showed higher fractionation.

Acknowledgements

References

[1] Zaman JA, Grace AA, Narayan SM. Future directions for mapping atrial fibrillation. Arrhythmia Electrophysiology Review 2022;11.

[2] Zeemering S, Van Hunnik A, Van Rosmalen F, Bonizzi P, Scaf B, Delhaas T, Verheule S, Schotten U. A novel tool for the identification and characterization of repetitive patterns in high-density contact mapping of atrial fibrillation. Frontiers in Physiology 2020;11:1304.

[3] Grace A, Willems S, Meyer C, Verma A, Heck P, Zhu M, Shi X, Chou D, Dang L, Scharf C, et al. High-resolution noncontact charge-density mapping of endocardial activation. JCI Insight 2019;4(6).

[4] Gharaviri A, Bidar E, Potse M, Zeemering S, Verheule S, Pezzuto S, et al. Epicardial fibrosis explains increased endo–epicardial dissociation and epicardial breakthroughs in human atrial fibrillation. Frontiers in Physiology 2020;11:68.

[5] van Rosmalen F, Maesen B, van Hunnik A, Hermans BJ, Bonizzi P, Bidar E, Nijs J, Maessen JG, Verheule S, Delhaas T, et al. Incidence, prevalence, and trajectories of repetitive conduction patterns in human atrial fibrillation. EP Europace 2021;23(Supplement_1):i123–i132.

[6] Wolf M, Tavernier R, Zeidan Z, El Haddad M, Vandekerckhove Y, Pooter JD, Phlips T, Strisciuglio T, Almorad A, Kyriakopoulou M, et al. Identification of repetitive atrial activation patterns in persistent atrial fibrillation by direct contact high-density electrogram mapping. Journal of Cardiovascular Electrophysiology 2019;30(12):2704–2712.

Address for correspondence:

Ozan Özgül
Universiteitssingel 50, UNS50, 6229 ER Maastricht, Netherlands
o.ozgul@maastrichtuniversity.nl